

Cell Reports Medicine, Volume 2

Supplemental information

**Functional diagnostics using fresh uncultured
lung tumor cells to guide personalized treatments**

Sarang S. Talwelkar, Mikko I. Mäyränpää, Lars Søråas, Swapnil Potdar, Jie Bao, Annabrita Hemmes, Nora Linnavirta, Jon Lømo, Jari Räsänen, Aija Knuuttila, Krister Wennerberg, and Emmy W. Verschuren

1 **Talwelkar et al.**

2 **Supplemental Information**

3

4 **Table of contents:**

5 **Supplementary Figure Legends**

6 ● **Figure S1.** Analysis of trametinib-induced signaling rewiring

7 ● **Figure S2.** Tumor tissue phenotyping and biochemical analysis of clinical samples

8 ● **Figure S3.** Drug response correlation to identify *KRAS*-mutant selective drug
9 sensitivities

10 ● **Figure S4.** Analysis of intratumoral genomic and phenotypic heterogeneity in a *KRAS*-
11 mutant lung cancer specimen

12 ● **Figure S5.** FUTC-based drug profiling identifies patient-selective drug sensitivities

13 ● **Figure S6.** Clinical response to carboplatin plus etoposide treatments

14

15 **Supplementary Table Legends**

16 ● **Table S1.** Clinical information of samples used for FUTC-based drug testing

17 ● **Table S2.** Immunohistochemical and phenotypic characterization of clinical lung
18 tumor tissues

19 ● **Table S3.** Identification of *KRAS*-selective drug sensitivities

20

21

22

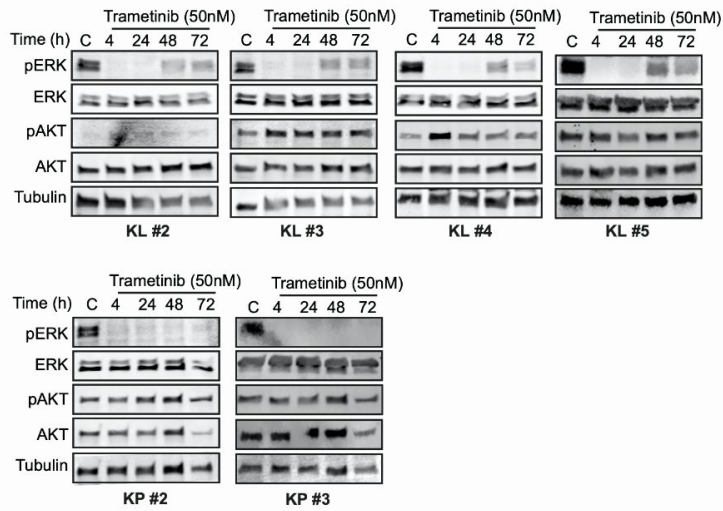
23

24

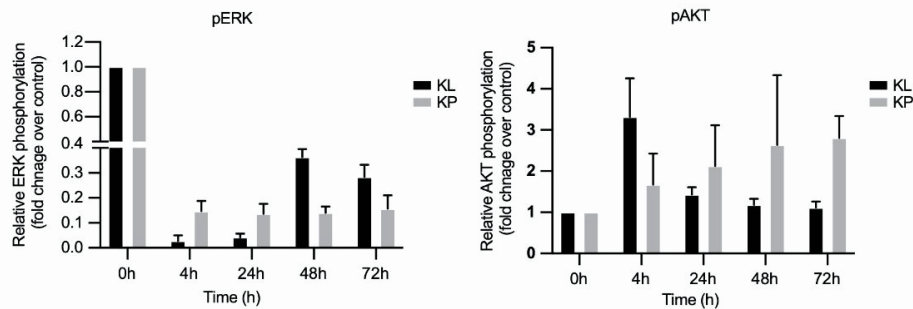
25 **Supplementary Figures**

Figure S1

A



B



26

27 **Figure S1. Analysis of trametinib-induced signaling rewiring. Related to Figure 2.** (A) Immunoblots of KL
 28 and KP FUTCs treated with vehicle (C; DMSO) and or treated with 50 nM TR for various time points (4, 24,
 29 48, and 72 h), and probed with indicated antibodies. (B) Relative quantification of pERK and pAKT signals on
 30 immunoblots presented in Figure 2D and S1A. Error bars represent ± SEM.

31

32

33

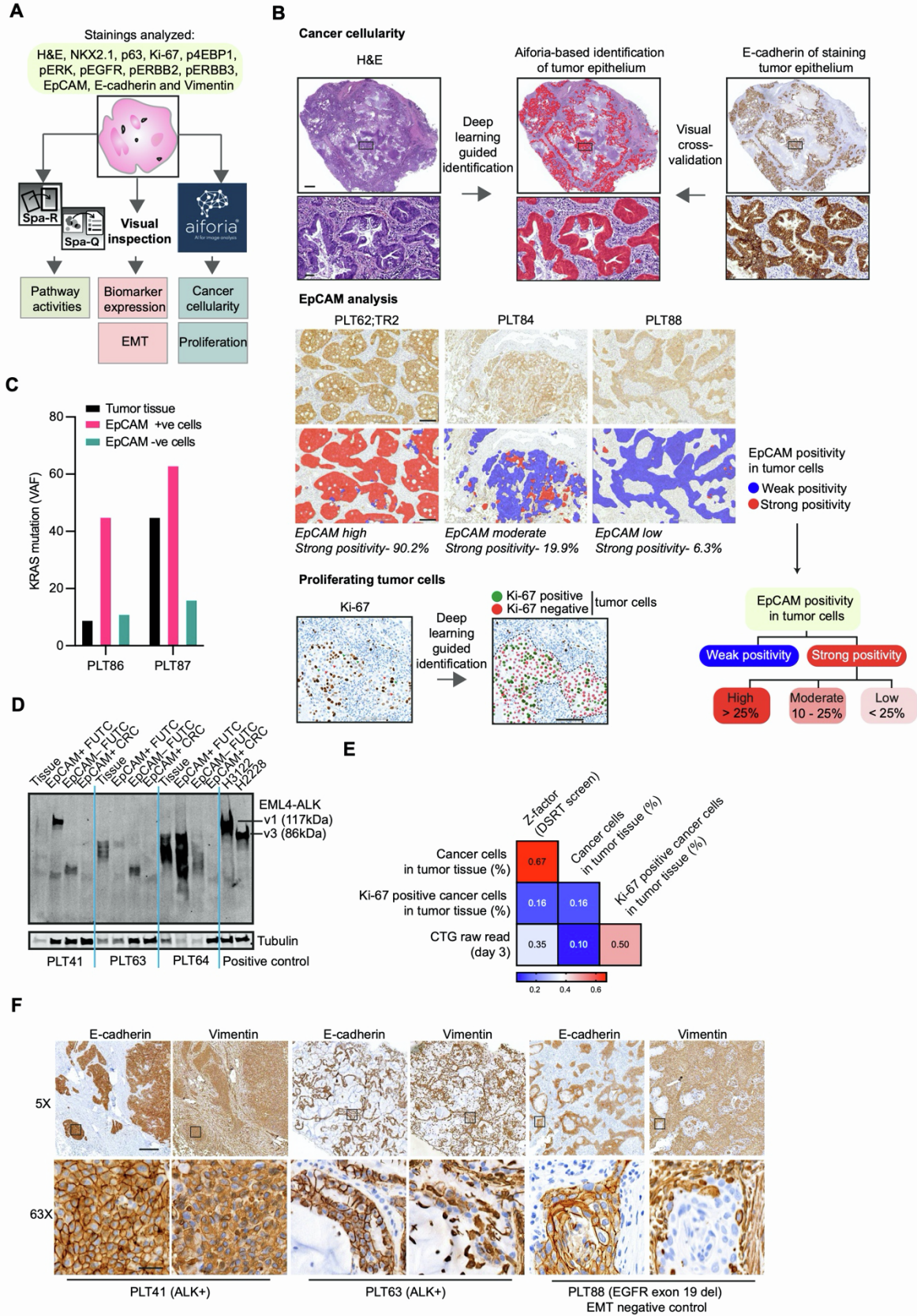
34

35

36

37

FIGURE S2



38

39 **Figure S2. Tumor tissue phenotyping and biochemical analysis of clinical samples. Related to Figure 3**
40 **and 4.** (A) The image analysis software package Spa-RQ⁵ was used for quantification of signaling activities in
41 tumor regions. To identify cancer cellularity, percentage of EpCAM positive cancer cells, and percentages of

42 Ki-67 positive proliferating cancer cells, deep learning-based Aiforia software was used. Biomarker expression
43 and EMT status was visually assessed for each tumor sample. (B) Top panel: representative images
44 demonstrating H&E staining (left), tumor epithelium identified using Aiforia (middle), and the validation via
45 epithelial staining of an adjacent tissue section stained with E-cadherin (right). Scale bars correspond to 1 mm or
46 50 μm for low or high magnifications, respectively. Middle panel: representative EpCAM stained images and
47 Aiforia-based detection of tumor cells exhibiting strong (red) and weak (blue) EpCAM positivity. Based on the
48 percentage of cancer cells exhibiting strong EpCAM positivity, samples were further subclassified into high (>
49 25%), moderate (10 - 25%), or low (< 10%). Scale bars correspond to 200 μm . Bottom panel: representative Ki-
50 67 stained images and Aiforia-based detection of Ki-67 positive (green) and negative (red) tumor cells. The
51 black dotted line indicates the edge of the tumor epithelium region identified by Aiforia in a separate analysis.
52 Scale bars correspond to 100 μm . (C) KRAS variant allele frequencies in tumor tissue and tumor-derived
53 EpCAM⁺ and EpCAM⁻ cells. (D) Immunoblot of EML4-ALK⁺ patient samples analyzed to verify the
54 expression of ALK fusion protein in patient-matched tumor tissue, tumor-derived EpCAM⁺ and EpCAM⁻ cells,
55 or CR cultures (passage #4). Samples from H3122 and H2228 cells (EML4-ALK⁺ cell lines) were used as
56 positive controls for v1 (117 kDa) and v3 (86 kDa) variants of EML4-ALK fusion proteins. (E) Heatmap
57 displaying Pearson correlation coefficient values between various factors associated with FUTC-based drug
58 testing. (F) Representative IHC images of E-cadherin and vimentin staining in patient-derived EML4-ALK⁺
59 lung tumor tissues. Scale bars correspond to 200 μm or 20 μm for low or high magnifications, respectively.
60 Boxes indicate areas depicted at higher magnification in the bottom row.

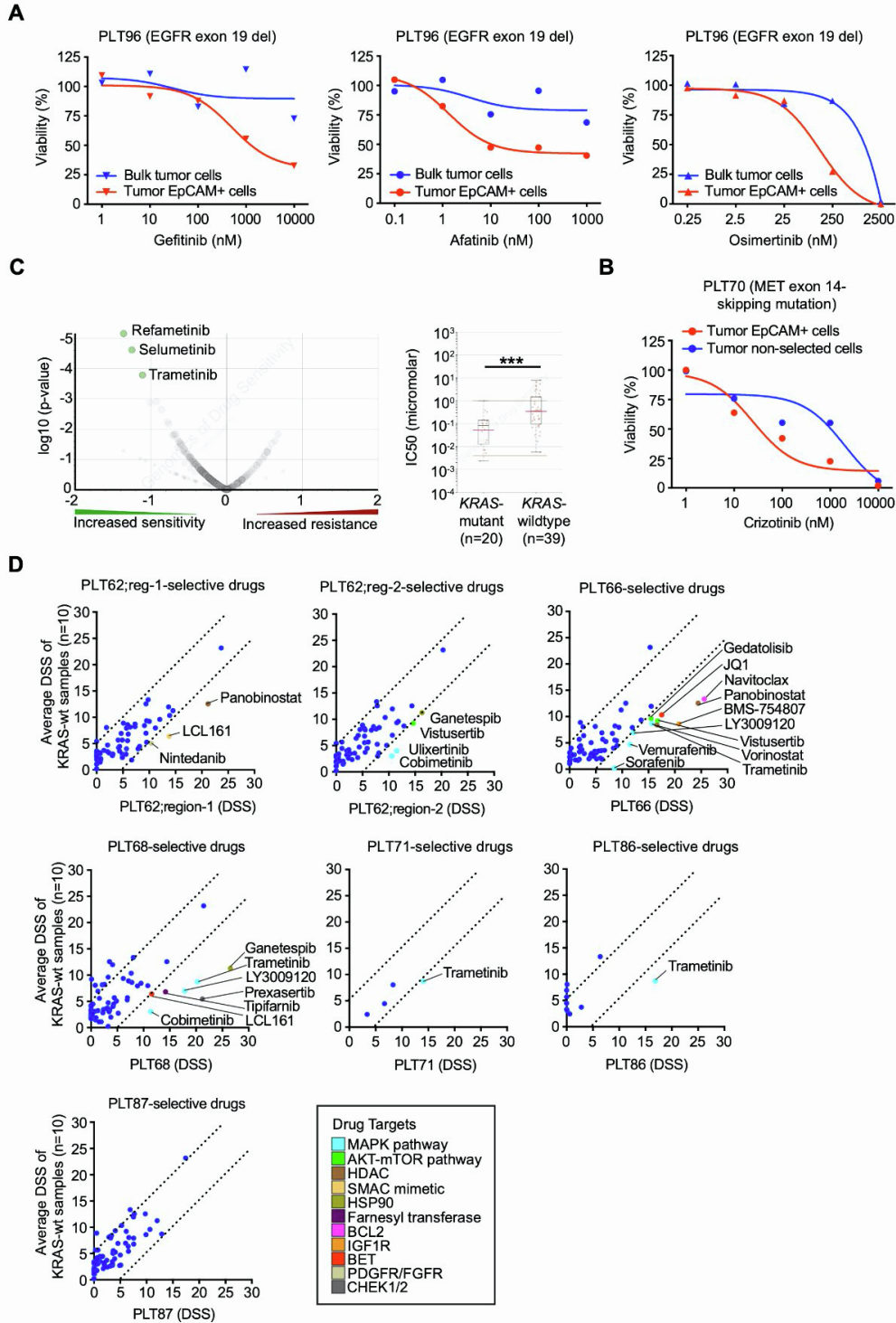
61

62

63

64

FIGURE S3

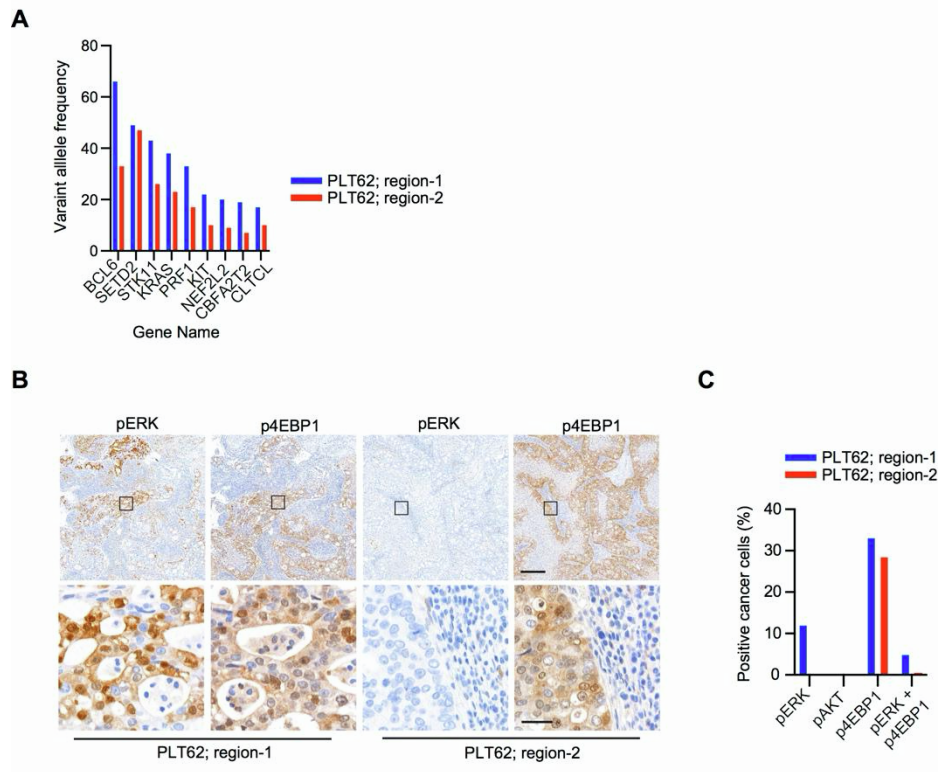


65

66 **Figure S3. Drug response correlation to identify *KRAS* mutant-selective drug sensitivities. Related to**
 67 **Figure 4 and 5. (A) Dose-response curves of gefitinib, osimertinib, and afatinib in patient-matched tumor-**
 68 **derived bulk cells and EpCAM+ cells. (B) Dose-response curves of crizotinib in patient-matched tumor-derived**
 69 **bulk cells and EpCAM+ cells. (C) A volcano plot (left) and box plot (right) representation adapted from**
 70 **Genomics of Drug Sensitivity in Cancer (GDSC1) database, showing association between MEK inhibitor**
 71 **sensitivity and *KRAS* mutation in lung adenocarcinoma cells. (D) Identification of patient-selective drug**
 72 **vulnerabilities by comparison of DSSs of individual *KRAS* mutant samples to average DSSs of *KRAS* wildtype**
 73 **samples (n=10). Drugs showing *KRAS* mutant sample-selective drug sensitivities (DSS difference >5) are color**
 74 **coded based on their target.**

75

FIGURE S4



76

77 **Figure S4. Analysis of intratumoral genomic and phenotypic heterogeneity in a *KRAS* mutant lung cancer**
 78 **specimens. Related to Figure 5.** (A) Bar graph displaying the variant allele frequencies of mutations
 79 normalized to percentages of cancer cells in their respective tumor region. (B) Representative IHC images of
 80 pERK, pAKT, p4EBP1 IHC staining in different regions of the PLT62 tissue sample. Scale bars correspond to
 81 200 μ m or 20 μ m for low or high magnifications, respectively. (C) Bar graph displaying levels of pERK
 82 (Thr202/Tyr204), pAKT (Ser473), p4EBP1 (Thr37/46) and overlapping phosphorylation of ERK and 4EBP1
 83 levels in cancer cells quantified using the IHC image registration and quantification tool, Spa-RQ.

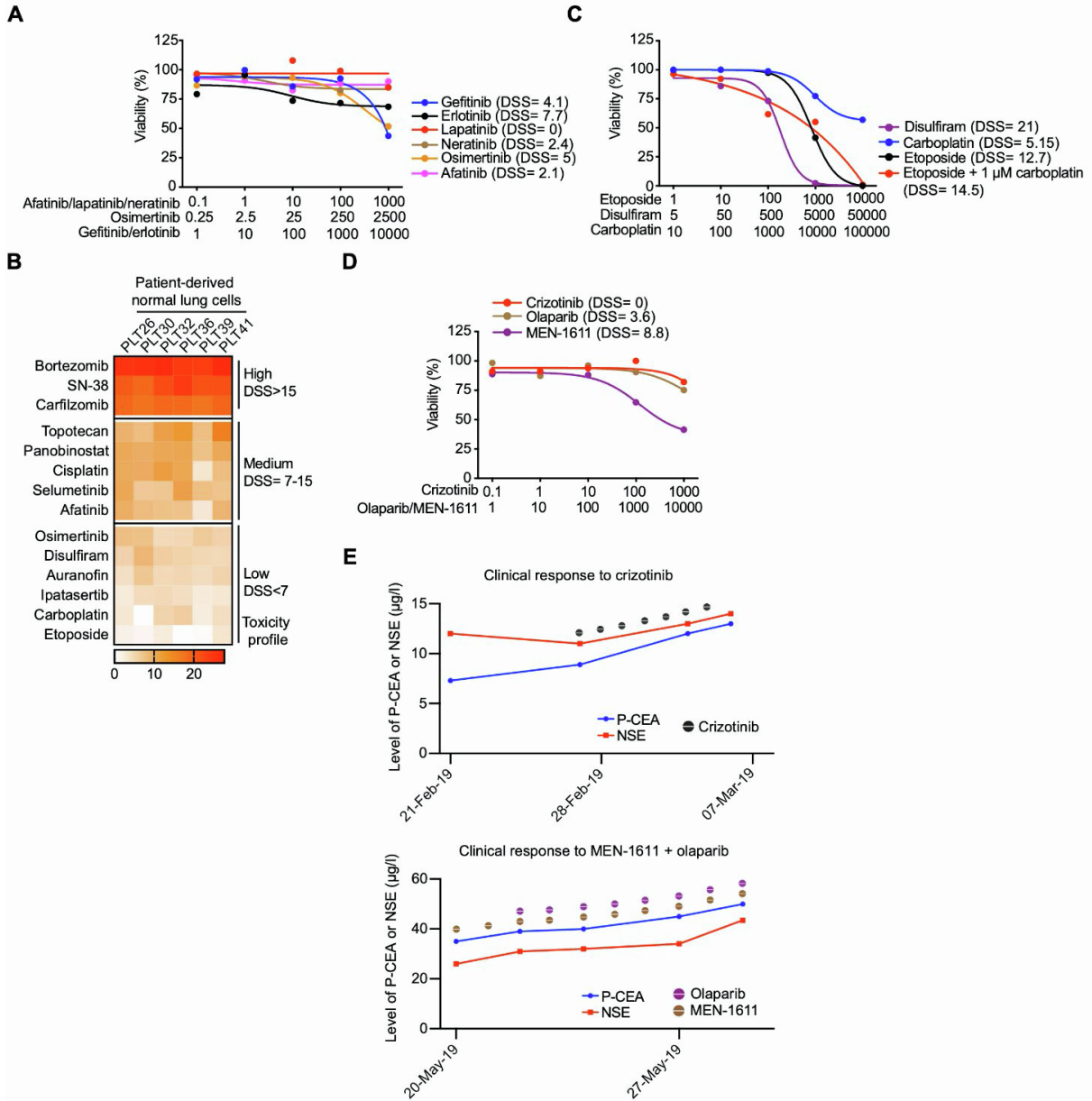
84

85

86

87

FIGURE S5



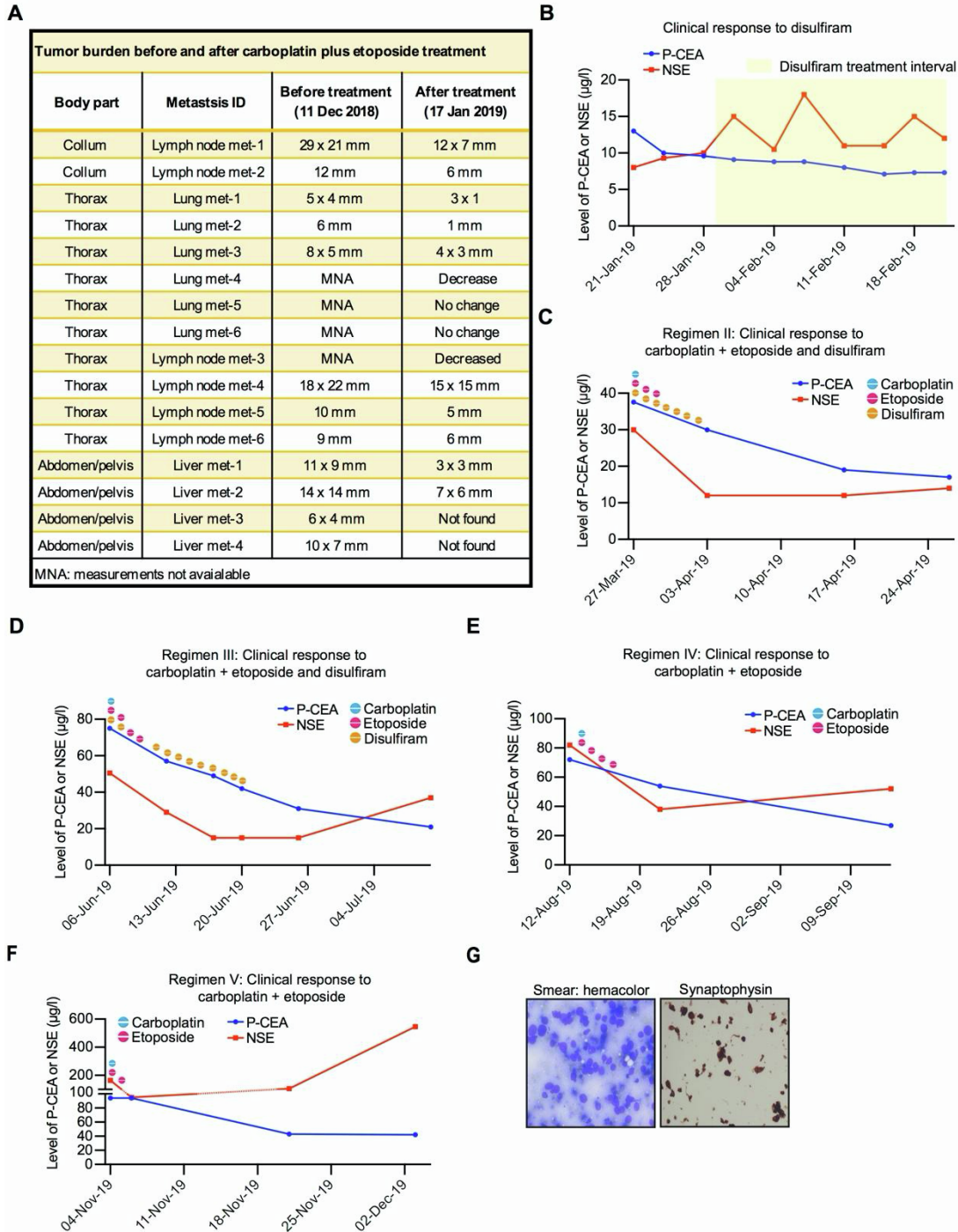
88

89 **Figure S5. FUTC-based drug profiling identifies patient-selective drug sensitivities. Related to Figure 6.**
 90 (A) Dose-response curves of different EGFR inhibitors in patient-derived FUTCs. (B) Toxicity profiles of top
 91 hits were assessed by testing their sensitivity in CR cultures established from healthy lung tissue of lung cancer
 92 patients. Drugs with average DSS >15 or DSS >7 are denoted as highly or mildly toxic, respectively. Drugs with
 93 average DSS <7 in the control cells were considered as putative lower toxicity compounds for clinical treatment.
 94 (C) Dose-response curves of patient-derived FUTCs treated with five doses of disulfiram, carboplatin,
 95 etoposide, and combination treatment. For the combination screen, 1 μM of carboplatin was used together with
 96 a dose series of etoposide. (D) Dose-response curves of patient-derived FUTCs treated with five doses of
 97 crizotinib, olaparib, and MEN-1611. (E) Changes in the level of CEA and NSE after treatment with crizotinib
 98 and MEN-1611 plus olaparib treatments.

99

100

FIGURE S6



101

102 **Figure S6. Clinical response to carboplatin plus etoposide treatments. Related to Figure 6.** (A) Effect of
 103 disulfiram and carboplatin plus etoposide treatment on size of metastatic lesions in lymph nodes, lung, and liver.
 104 (B) Changes in the level of CEA and NSE after disulfiram treatments. (C-F) Changes in the level of CEA and
 105 NSE after carboplatin plus etoposide treatments with or without disulfiram. (G) Hemacolor stained (left) and
 106 synaptophysin (right) stains of cell smear obtained from a fine needle aspiration from a lymph node biopsy
 107 (collected in Jan 2020).

108

109

110

111 **Table S1**

Table S1 Clinical information of samples used for FUTC-based drug testing. Related to Figure 3.

Sample ID	Gender/age	Lung cancer	TNM stage	Oncogenic driver	Treatment	Smoking history	Tumor location
PLT37	F/73	SCC	T1bN0M0	nd	surgery	2	Left lower lobe
PLT38	M/57	AC	T3N1M0	uod	surgery	0	Left upper lobe
PLT39	M/66	MAC	results not available	uod	surgery	0	Right upper lobe
PLT41	M/56	AC	solitary recurr in mediastinum	ALK fusion +	surgery	0	Mediastinum
PLT62	F/50	AC	T2aN1M0	KRAS G13D	surgery + chemotherapy	2	Right lower lobe
PLT63	F/68	AC	T3N0M0	ALK fusion +	surgery	1	Left upper lobe
PLT64	F/25	AC	T2aN1M0	ALK fusion +	surgery + chemotherapy	0	Left lower lobe
PLT66	M/71	AC	T3N0M0	KRAS G12C	surgery	2	Right lower lobe
PLT68	F/68	AC	T1cN0M0	KRAS G12S	surgery	1	Right lower lobe
PLT70	M/82	AC	T1cN0M0	MET exon 14 skipping mutation	surgery	0	Right upper lobe
PLT71	F/58	AC	T2N0M0	KRAS G12V	surgery	2	Right lower lobe
PLT72	M/70	AC	T2bN0M0	EGFR L858R	surgery	1	Right upper lobe
PLT84	M/60	AC	T2N2M0	EGFR exon 19 del	surgery + adjuv. chemotherapy	0	Right upper lobe
PLT85	F/76	AC	T2aN0M0	EGFR L858R	surgery	0	Right upper lobe
PLT86	F/68	AC	T2N0M0	KRAS G12V	surgery + adjuv. chemotherapy	0	Right upper lobe
PLT87	F/61	AC	T3N0M0	KRAS G12C	surgery	2	Right lower lobe
PLT88	F/43	ASC	T2bN1M0	EGFR exon 19 del and EGFR amp	surgery + postop. chemoradiotherapy	0	Right upper lobe

SCC: squamous cell carcinoma, AC: adenocarcinoma, MAC: mucinous adenocarcinoma, ASC: adenosquamous carcinoma, nd: not done, uod: unknown oncogenic driver, never smoker: 0, ex-smoker: 1, current smoker: 2

112

113

114

115

116

117

118

119

120

121

122

123

124

125

126

127

128

129

130

131

132

133

134

135 **Table S2**

Table S2 Immunohistochemical and phenotypic characterization of clinical lung tumor tissues. Related to Figure 3, Figure 4 and Figure 5.

Sample ID	Lung cancer type	Tumor epithelial region (%)	EpCAM+ cells normalized to total cancer cells (%): strong positivity	EpCAM+ cells normalized to total cancer cells (%): weak positivity	Ki-67+ cells normalized to total cancer cells (%)	p4EBP1+ cells normalized to total cancer cells (%)	pERK+ cells normalized to total cancer cells (%)	pERK and p4EBP1 double positive cells normalized to total cancer	pEGFR positive cancer cells	pERBB2 positive cancer cells	pERBB3 positive cancer cells	E-cadherin and vimentin double positive cells
PLT37	SCC	28.15	26.35	73.65	39.82	10.25	0.00	0.00	-	-	-	-
PLT38	AC	14.3	46.85	53.15	39.32	13.58	1.47	1.03	-	-	-	-
PLT39	MAC	4.754	29.79	70.21	15.85	1.46	3.42	0.09	-	-	-	-
PLT41	AC	46.56	6.71	93.29	10.85	0.33	0.00	0.00	nd	nd	nd	+
PLT62; region1	AC	42.33	77.29	22.71	29.91	33.31	12.21	5.10	+	-	-	-
PLT62; region2	AC	49.69	90.23	7.77	32.31	28.69	0.00	0.00	+	-	-	-
PLT63	AC	21.8	18.05	81.95	9.77	9.30	5.91	0.65	-	-	-	+
PLT64	AC	47.3	2.795	97.205	16.26	3.51	0.00	0.00	-	-	-	+
PLT66	AC	16.68	54.6	45.4	23.71	1.19	47.56	0.47	-	-	-	-
PLT68	AC	38.07	63.61	36.39	24.69	0.09	27.13	0.01	-	-	-	-
PLT70	AC	21.14	32.53	67.47	4.28	0.30	0.00	0.00	-	-	-	-
PLT71	AC	10.84	29.43	70.57	49.58	2.47	7.17	0.18	+	-	-	-
PLT72	AC	22.51	1.67	98.33	11.11	3.46	0.00	0.88	-	-	-	+
PLT84	AC	17.73	19.97	80.03	5.82	13.85	42.23	6.32	+	+	+	+
PLT85	AC	2.574	45.09	54.01	4.39	13.96	69.05	7.79	+	+	+	-
PLT86	AC	12.99	70.57	29.43	17.45	45.18	71.58	6.46	-	-	-	-
PLT87	AC	61.15	86.99	13.01	65.42	7.44	23.24	2.41	+	+	-	-
PLT88	ASC	22.55	6.39	93.61	27.94	0.08	0.00	0.00	+	+	+	+
PLT 96	AC	12.39	30.64	69.36	10.89	nd	nd	nd	nd	nd	nd	nd

SCC: squamous cell carcinoma, AC: adenocarcinoma, MAC: mucinous adenocarcinoma, ASC: adenosquamous carcinoma, + : present, - : absent, nd: not done

136

137

138

139

140

141

142

143

144

145

146

147

148

149

150

151

152

153

154

155

156

157

Table S3 DSS comparison between KRAS mutant cells and KRAS wildtype cells for 66 oncology drugs . Related to Figure 5.

KRAS-selective hit ID	Drug Name	Mean Diff	Median Diff	p.val	adjusted Pval	t.test	t.adjust
1	Trametinib	8.060	7.850	0.004	0.262	0.001	0.072
2	Panobinostat	4.633	1.350	0.268	0.937	0.245	0.737
3	LY3009120	4.227	2.600	0.149	0.937	0.114	0.737
4	Ganetespib	3.884	2.300	0.745	0.958	0.424	0.737
5	Cobimetinib	3.103	0.100	0.329	0.937	0.199	0.737
6	Ulixertinib	2.573	4.400	0.191	0.937	0.370	0.737
7	Sorafenib	2.083	0.000	0.353	0.937	0.280	0.737
8	Ravoxertinib	1.577	1.500	0.254	0.937	0.349	0.737
9	Olaparib	1.504	1.400	0.074	0.809	0.188	0.737
10	Gandotinib	1.366	3.000	0.415	0.937	0.376	0.737
11	Prexasertib	1.340	2.850	1.000	1.000	0.771	0.950
12	Nintedanib	1.217	1.750	0.432	0.937	0.610	0.895
13	Afatinib	1.005	5.900	0.356	0.937	0.673	0.907
14	Tipifarnib	0.996	1.150	0.745	0.958	0.652	0.906
15	LCL161	0.963	3.600	0.569	0.937	0.801	0.950
16	Vorinostat	0.821	0.700	0.876	1.000	0.761	0.950
17	Vismodegib	0.707	0.950	0.501	0.937	0.727	0.941
18	Gedatolisib	0.683	1.900	0.755	0.958	0.837	0.950
19	BMS-754807	0.669	0.050	0.935	1.000	0.848	0.950
20	JQ1	0.363	-1.300	1.000	1.000	0.914	0.955
21	Vemurafenib	0.057	-1.200	1.000	1.000	0.982	0.982
22	Dabrafenib	-0.151	0.700	0.563	0.937	0.926	0.955
23	Doxorubicin	-0.244	3.000	0.639	0.937	0.946	0.961
24	AZD4547	-0.257	0.400	1.000	1.000	0.860	0.950
25	Carboplatin	-0.297	-0.100	1.000	1.000	0.856	0.950
26	Dasatinib	-0.314	-0.050	1.000	1.000	0.896	0.955
27	Roxadustat	-0.324	-0.200	1.000	1.000	0.864	0.950
28	Vistusertib	-0.417	-2.000	1.000	1.000	0.912	0.955
29	Chloroquine	-0.500	-1.550	1.000	1.000	0.808	0.950
30	PAC-1	-0.531	-0.400	0.807	0.987	0.659	0.906
31	TAK-715	-0.796	-2.150	0.508	0.937	0.574	0.876
32	Sonidegib	-0.881	0.000	0.440	0.937	0.315	0.737
33	Perifosine	-0.884	-0.750	0.456	0.937	0.296	0.737
34	Alpelisib	-0.920	-1.200	0.394	0.937	0.391	0.737
35	Metformin	-0.923	-0.500	0.238	0.937	0.183	0.737
36	Foretinib	-1.003	-1.450	0.608	0.937	0.447	0.737
37	Docetaxel	-1.027	1.550	0.684	0.958	0.647	0.906
38	KU-60019	-1.030	-0.100	0.522	0.937	0.284	0.737
39	Volasertib	-1.126	-1.100	0.102	0.937	0.062	0.737
40	Cabozantinib	-1.130	0.600	0.934	1.000	0.416	0.737
41	Ipatasertib	-1.176	-2.600	0.755	0.958	0.704	0.929
42	Ponatinib	-1.287	-0.475	0.628	0.937	0.444	0.737
43	Palbociclib	-1.303	-1.300	0.515	0.937	0.472	0.760
44	Veliparib	-1.320	-0.700	0.463	0.937	0.264	0.737
45	Osimertinib	-1.428	-0.950	0.518	0.937	0.446	0.737
46	Dexamethasone	-1.487	0.000	0.717	0.958	0.370	0.737
47	Birabresib	-1.664	-2.000	0.639	0.937	0.584	0.876
48	Gefitinib	-1.677	1.300	0.792	0.987	0.389	0.737
49	Dovitinib	-1.711	-0.200	0.741	0.958	0.389	0.737
50	Lapatinib	-1.743	-0.100	0.066	0.809	0.250	0.737
51	NVP-LGK974	-1.813	-1.550	0.623	0.937	0.217	0.737
52	Gemcitabine	-1.888	-2.275	0.429	0.937	0.186	0.737
53	Crizotinib	-1.902	-2.700	0.136	0.937	0.069	0.737
54	Ralimetinib	-1.971	-1.550	0.515	0.937	0.255	0.737
55	VE-821	-2.069	-1.400	0.260	0.937	0.070	0.737
56	Ruxolitinib	-2.171	-1.100	0.624	0.937	0.330	0.737
57	Ceritinib	-2.492	-1.725	0.228	0.937	0.201	0.737
58	Pomalidomide	-2.869	-2.000	0.116	0.937	0.182	0.737
59	Vincristine	-2.994	-1.700	0.326	0.937	0.155	0.737
60	Azacitidine	-3.344	-3.650	0.073	0.809	0.069	0.737
61	Navitoclax	-3.365	-5.325	0.628	0.937	0.486	0.764
62	Dinaciclib	-3.503	-7.100	0.432	0.937	0.438	0.737
63	Everolimus	-3.991	-4.000	0.074	0.809	0.061	0.737
64	Pictilisib	-4.691	0.000	0.569	0.937	0.155	0.737
65	Idasanutlin	-4.938	-7.300	0.202	0.937	0.082	0.737
66	Cisplatin	-5.811	-1.300	0.074	0.809	0.117	0.737

160 **References**

- 161 1. Talwelkar SS, Nagaraj AS, Devlin JR, Hemmes A, Potdar S, Kiss EA, et al. Receptor
162 Tyrosine Kinase Signaling Networks Define Sensitivity to ERBB Inhibition and
163 Stratify Kras-Mutant Lung Cancers. *Molecular cancer therapeutics*. 2019;18(10):1863-
164 74.
- 165 2. Potdar S, Ianevski A, Mpindi JP, Bychkov D, Fiere C, Ianevski P, et al. Breeze: an
166 integrated quality control and data analysis application for high-throughput drug
167 screening. *Bioinformatics*. 2020.
- 168 3. Yadav B, Pemovska T, Szwajda A, Kuleskiy E, Kontro M, Karjalainen R, et al.
169 Quantitative scoring of differential drug sensitivity for individually optimized
170 anticancer therapies. *Sci Rep*. 2014;4:5193.
- 171 4. Dufva O, Kankainen M, Kelkka T, Sekiguchi N, Awad SA, Eldfors S, et al. Aggressive
172 natural killer-cell leukemia mutational landscape and drug profiling highlight JAK-
173 STAT signaling as therapeutic target. *Nat Commun*. 2018;9(1):1567.
- 174 5. Bao J, Walliander M, Kovacs F, Nagaraj AS, Hemmes A, Sarhadi VK, et al. Spa-RQ:
175 an Image Analysis Tool to Visualise and Quantify Spatial Phenotypes Applied to Non-
176 Small Cell Lung Cancer. *Sci Rep*. 2019;9(1):17613.
- 177